

Constitutive model coupled with damage for carbon manganese steel in low cycle fatigue

Zhiyong Huang^{*1}, Qingyuan Wang¹, Danièle Wagner² and Claude Bathias²

¹ School of Aeronautics and Astronautics, Sichuan University,
No. 29 Jiuyanqiao Wangjiang Road, Chengdu, 610064, China

² Université ParisOvest Nanterre La Défense, 50 rue de Sèvres, Ville d'avray, 92410, France

(Received February 03, 2014, Revised June 10, 2014, Accepted July 01, 2014)

Abstract. Carbon-manganese steel A42 (French standards) is used in steam generator pipes of nuclear center and subject to low cycle fatigue (LCF) loads. In order to obtain the material LCF behavior, the tests are implemented in a hydraulic fatigue machine. The LCF plastic deformation and cyclic stress in macroscope have been influenced by the accumulated low cycle fatigue damage. The constitutive kinematic and isotropic hardening modeling is modified with coupling fatigue damage to describe the fatigue behavior. The improved model seems to be good agreement with the test results.

Keywords: low cycle fatigue; fatigue damage; carbon manganese steel; plastic deformation

1. Introduction

Some cases of Pressurized Water Reactor (PWR) components are suffered Low Cycle Fatigue (LCF) load induced by mixing of cold and hot fluids as introduced in the report of Le Duff (2009). The fatigue damage in PWR components caused by thermal stratification in secondary feedwater lines has been observed by Huang (2011) in nuclear power plant. LCF loads are due to layered cold and hot water in horizontal parts of the feed water lines; loads correspond to the case linked to variations of temperature with low frequency. The American Society of Mechanical Engineers (ASME) Boiler and Pressure Vessel Code Section III, subsection NB, containing rules of design for nuclear power plants, recognizes fatigue as a possible mode of failure in pressure vessel steels and piping materials as reported by Chopra (2002).

The components are subject to a large number of cycles and the primary concerning is the endurance limit. Cyclic loading on a reactor pressure component occurs because of the mechanical and thermal loading as the system going from one load set (e.g., pressure, temperature, moment, and force loading) to another. The number of cycles applied during the design life of the component seldom exceeds 105 cycles and is typically less than a few thousands (e.g., low cycle

*Corresponding author, Ph.D., E-mail: huangzy@scu.edu.cn

^a Professor

^b Doctor

^c Professor

fatigue). The main difference between HCF and LCF is the former involves little or no plastic strain in macroscope, whereas the latter involves plastic strain. Therefore, design curves for low cycle fatigue are found on test results where strain rather than stress is controlled.

Two nonlinear hardening behaviors called kinematic hardening and isotropic hardening appear in the LCF. Model proposed by Armstrong and Frederick (1966) improved by Chaboche (2008), Ohno (2013) is often used to describe the material constitutive relation of cyclic strain-stress hysteresis loops with Bauschinger effect. The cyclic isotropy hardness law presents the cyclic stress amplitude rising with number of cycles increasing. The fatigue damage can be described by continuum damage mechanics (CDM) proposed by Rabotnov (1969), and developed by Lemaitre (1990) and Chaboche (1987, 2009). It gave out the theoretical preparation by derivation the differential form of damage in the framework of thermodynamics. The stress amplitude in LCF is not constant in the strain controlled mode caused by cyclic hardening and the fatigue damage. The kinematic and isotropic hardening is responsible for the stress amplitude increasing in the beginning of the fatigue test, and the fatigue damage is responsible for the decline of stress amplitude before the failure.

The fatigue damage affects on the fatigue behavior with cycles rising, and it is necessary to be introduced into the constitutive model in LCF. In terms of the framework of thermodynamic, the improved constitutive model coupled with fatigue damage model is proposed and the cyclic stress and plastic deformation are estimated by implicit integrated method and verified by the test results.

2. Material and tests

One of the materials of feedwater lines in French nuclear power plants widely used is A42, low carbon manganese steel, AFNOR NFA 36205(French Standard). The material was received as 40 mm thick plates sustained a prior normalization heat treatment consisted of austenitising at 870°C followed by air cooling, leading to a microstructure composed by ferritic and pearlitic bands (Fig. 1).

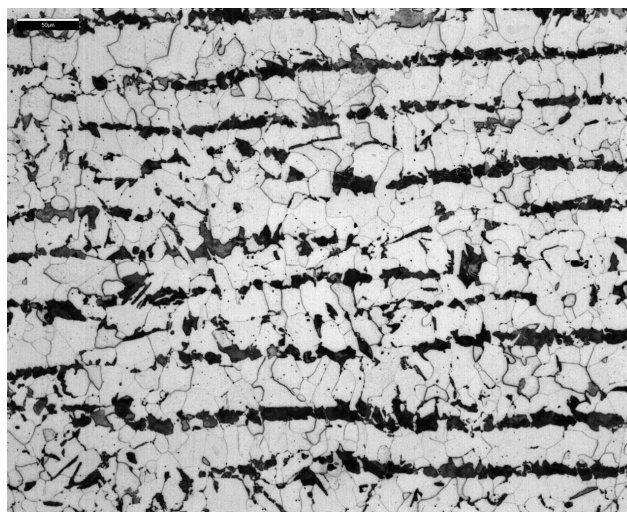


Fig. 1 Steel A42 optical microscope

Table 1 Chemical composition of A42 (wt%)

C	S	P	Si	Mn	Ni	Cr
0.140	0.0057	0.016	0.225	0.989	0.024	0.021
Mo	Cu	Sn	Al	N	O	Mo
0.002	0.027	0.003	0.045	0.0082	0.0006	0.002

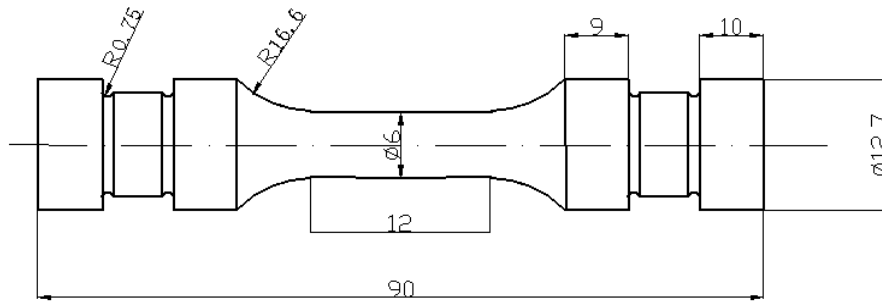


Fig. 2 Schematic illustration of low cycle fatigue specimen

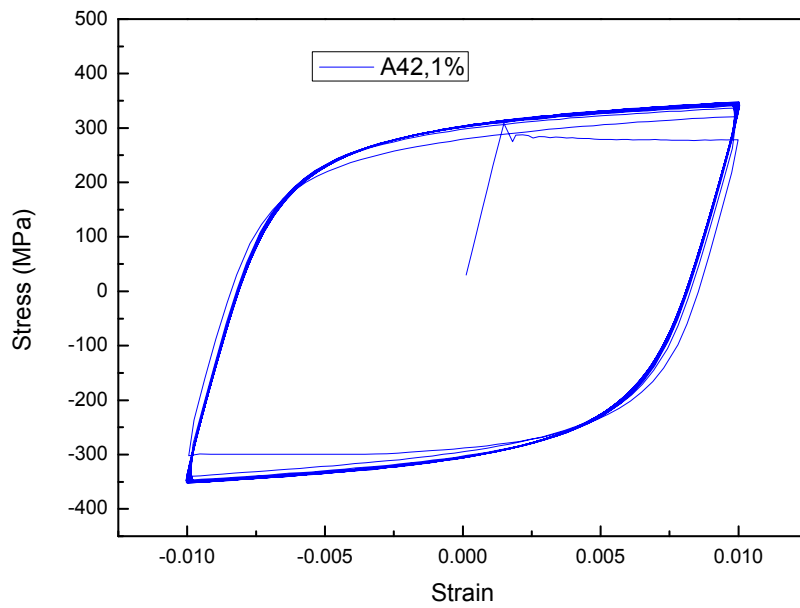


Fig. 3 Hysteresis loops in 1% strain amplitude for A42 (0.1 Hz, RT)

Low cycle fatigue machine Instron 8501 has been calibrated before testing. Low cycle fatigue specimens were designed as Fig. 2 illustrated. In the middle of the specimen, test region has been reserved as 12 mm in length, 10 mm in diameter cylinder for installing extensometer which is bound to the surface of specimen by two springs or two plastic rings and is controlled by computer with standard serial interface. At each end of the specimen, a reduction shape is designed to adapt the clamps of the low cycle fatigue machine.

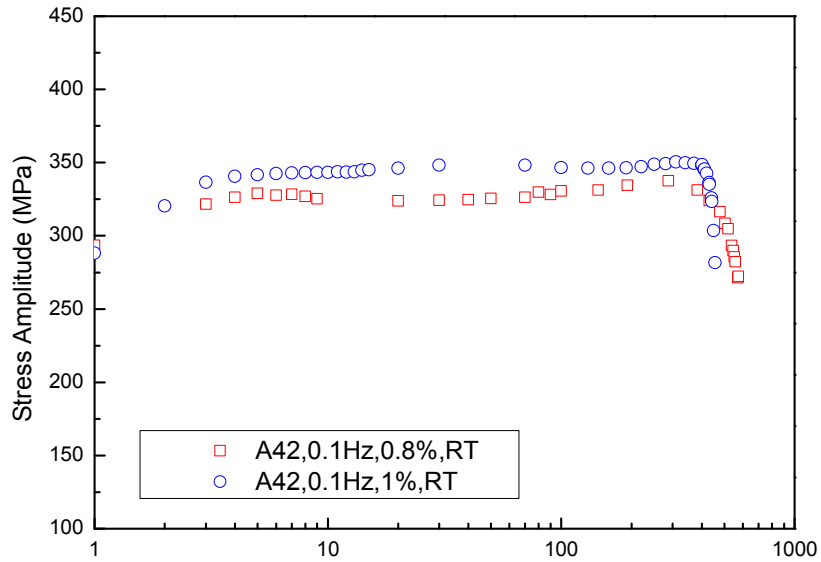


Fig. 4 Cyclic stress evolutions for 0.8% and 1% strain amplitude (A42, RT)

The Fig. 3 is the LCF test hysteresis loops for A42 with 1% strain amplitude, 0.1 Hz test frequency in room temperature. The first quarter cyclic stress-strain curve, under uniaxial tension of the C-Mn steel, yield phenomena characterized by a high sharp yield point followed by a subsequent yield drop and a relative plateau are observed, where a localized plastic deformation

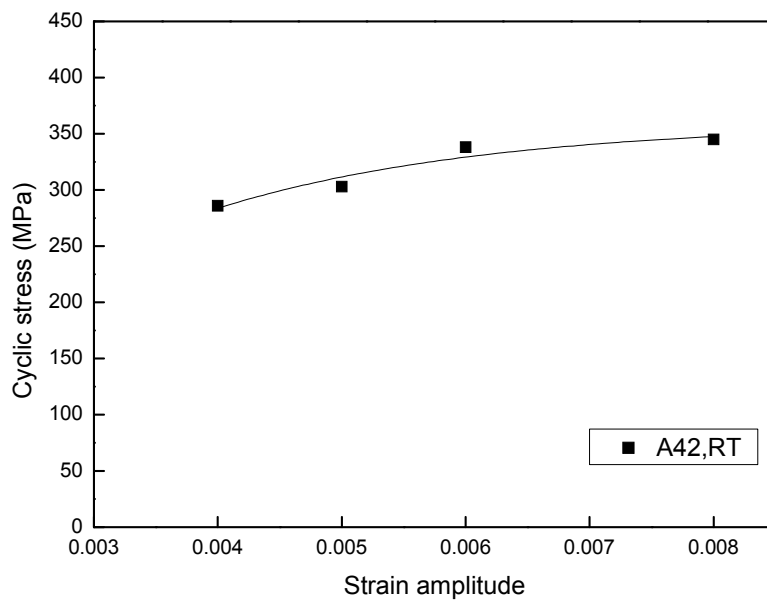


Fig. 5 Cyclic stress versus strain amplitude

appears as a result of Lüders-bands propagation under a constant lower yield stress. The Lüders strain also depends on the length of testing region of the specimen. In the first cycle of low cycle fatigue test, after the traction over, the subsequent compression is loaded to the specimen and the so called Bauschinger effect appears: with the greater tensile cold working, the compressive yield strength is lowered.

The stress amplitude increasing is remarkable in the first several cycles caused by the isotropic hardening. Especially, the second cycle hardening is significant, through the observation of the Fig. 3 for A42 steel.

Fig. 4 denotes the stress amplitude evolutions during reversed cyclic load with 0.1 Hz frequency for A42. The square points indicate that the 1% strain amplitude hardening is more pronounced than 0.8%. In this case, the cyclic stress reached to 350 MPa in cyclic stabilization for 1% strain amplitude and the stress appears to drop after about 300 cycles. For 0.8% strain amplitude with round points in Fig. 4, the stress keeps almost at 320 MPa before dropping. The stress evolution drop is caused by the fatigue damage and the fatigue crack appears and propagates in the period. The following chapter will model the evolution with the help of the constitutive relation coupled with fatigue damage.

The stress amplitude of middle life of LCF fatigue tests varying with strain amplitude in LCF is shown in Fig. 5. The fatigue cycles hardened the A42 steel in LCF. The fatigue cyclic constitutive relationship is described by the formula: $\sigma_a = K \varepsilon_a^n$, ($n = 0.2544$, $K = 118$ MPa).

3. Constitutive relation coupled with fatigue damage

3.1 Thermodynamic framework

In LCF, plastic deformation forms hysteresis loops. Armstrong and Frederick (A-F) gave out a non linear kinematic hardening model formulated by a serial of differential equations. They introduced the concept of strain hardening and dynamic recovery to specify the back stress. Chaboche *et al.* (2009) extended it by decomposing the back stress into many components in order to describe constitutive relationship more precisely. The parameters of the model are identified from the hysteresis loop and the stress amplitude evolution in LCF. The kinematic hardening is comprised of the thermodynamic framework which is explained by Lemaitre and Chaboche (1990). Some internal variables are used to describe the irreversible processes. The theory is applied for small quasi static transformations, using T for the temperature, ε_e for elastic strain tensor, a_j for the family of internal variables that express the current state of the material. Two potential functions are used, thermodynamic potential (ψ) and dissipation potential (φ^*) expressed as follows

$$\psi = \psi(\varepsilon_e, T, \alpha_i) \quad (1)$$

$$\varphi^* = \varphi^*(\sigma, A_j, \varepsilon_e, T, a_j) \quad (2)$$

ψ , φ^* are potential functions which are assumed as follows

$$\rho\psi = \frac{1}{2} D_e : \varepsilon^e : \varepsilon^e + \frac{1}{3} ha : a + W(r, T) \quad (3)$$

$$\varphi^* = g = g\left(J(\sigma - \alpha) - R - k + \frac{3\zeta}{4h} a:\alpha\right) = g\left(f + \frac{3\zeta}{4h} a:\alpha\right) \quad (4)$$

The mechanical variables are deduced from the functions based on the second law of thermodynamics; the above energy leads to

$$\sigma = \rho \frac{\partial \psi}{\partial \varepsilon^e}, \quad S = -\frac{\partial \psi}{\partial T}, \quad A_j = \rho \frac{\partial \psi}{\partial a_j} \quad (5)$$

$$\dot{\varepsilon}^p = \frac{\partial \varphi^*}{\partial \sigma}, \quad \dot{a}_j = -\frac{\partial \varphi^*}{\partial A_j} \quad (6)$$

Where a is the internal “strain variable” associated with the center α of the elastic domain, r is the isotropic variable, associated with R . D_e is the elastic matrix.

3.2 LCF Damage

The micro defects nucleation process, growth and merging under reversed loading lead to the initiation of crack and induce progressive weakness of material toughness and stiffness. It is considered as a damage evolution. The state of damage in the material, D , is theoretically determined by the common influence of size and configuration of microcracks and microvoids. The effective macroscopic stress $\tilde{\sigma}$ within the damaged material is determined by assuming that the nominal cross section A was reduced by the size of the damaged area A_D and the damage is defined as: $D = \frac{A_D}{A}$.

So the effective stress is

$$\tilde{\sigma} = \frac{F}{A - A_D} = \frac{F/A}{1 - A_D/A} = \frac{\sigma}{1 - D} \quad (7)$$

The damage in general theory is a function of time, deformation and stress. In the case of fatigue, we employ the notion of loading cycles for identifying the damage evolution and measuring the fatigue life. The evolution of fatigue damage is taken as the form: $\delta D = F(\dots) \delta N$. F is the function of the variables like state parameters (temperature, damage, cyclic hardening, etc.), load definition parameters (stress, strain or plastic strain, strain or stress ratio).

The prior cyclic load has damage effect on the subsequent loading for real nuclear pipes. Two levels cumulative damage model is proposed by Chaboche *et al.* (2009) as follows

$$\frac{dD}{dN} = \frac{D^\alpha}{(1 - \alpha) N_f(\sigma_a)} = \frac{D^\alpha}{N_f^*(\sigma_a)} \quad (8)$$

The function $N_f(\sigma_a)$ is the function chosen for the Wöhler curve, taken as a power function. The stress amplitude σ_a could be in LCF, HCF and VHCF load. One group of parameters of Basquin’s model is hard to describe 3 regime fatigue behaviors. In order to describe S-N curve at LCF, HCF and VHCF, the multi group parameters of Basquin model are applied for S-N curve with $N_f(\sigma_{a_{eff}})$ and hidden function $N_f^*(\sigma_{a_{eff}})$.

$$N_{fi}(\sigma_{ia}) = \left(\frac{\sigma_{ia}}{M_i} \right)^{-\gamma_i}, \quad N_{fi}^*(\sigma_{ia}) = \left(\frac{\sigma_{ia}}{M_i^*} \right)^{-\beta_i^*} \quad (i = 1, 2, 3) \quad (9)$$

where $\beta_i^* = \theta_i \gamma_i$, θ_i ($i = 1, 2, 3$) are the additional parameters. Subscript $i = 1, 2, 3$ expresses LCF, HCF and VHCF regime respectively. Please note that parameters M_i^* never play role in the results for multilevel fatigue tests within a regime. Equality of both sides of Eq. (9) automatically

gives the function α : $1 - \alpha = \frac{N_f^*(\sigma_a)}{N_f(\sigma_a)}$

Using N/N_f to identify the fatigue damage can induce an indetermination as a little change of the α in D^α which will affect a lot to the value of damage. In the case of one level load and one-dimensional damage, the differential Eq. (9) is given out for the reversed loading conditions without considering mean stress effect. In order to combine the evaluations with the corresponding remain life, the defined damage D is replaced by $1 - (1 - D)^{\beta+1}$ and the damage can be given out

$$\frac{dD}{dN} = \left[1 - (1 - D)^{\beta+1} \right]^{\alpha(\sigma_a)} \left[\frac{\sigma_a - \sigma_{t_0}}{M(1 - D)} \right]^\beta \quad (10)$$

The damage can be written with the variable N/N_f

$$D = 1 - \left[1 - \left(\frac{N}{N_f} \right)^{\frac{1}{1-\alpha}} \right]^{\frac{1}{\beta+1}} \quad (11)$$

Where, $\alpha(\sigma_a) = 1 - a \left\langle \frac{\sigma_a - \sigma_F}{\sigma_u - \sigma_a} \right\rangle$.

σ_F is fatigue limit; σ_u is static fracture strength; M and β are the parameters of S-N curve. In the case of LCF, the cyclic stress can be replaced by cyclic strain: $\sigma_a = K \varepsilon_a^n$. So the σ_a replaced by

ε_a , like $\alpha(\varepsilon_a) = 1 - a \left\langle \frac{K \varepsilon_a^n - \sigma_F}{\sigma_u - K \varepsilon_a^n} \right\rangle$.

3.3 LCF damage plasticity coupling with damage

In the process of LCF, the damage is related with cumulative plastic deformation closely and influences the fatigue behavior. The damage variable D is necessary to be introduced into the constitutive relation. The total strain is consisted of elastic and plastic parts

$$\varepsilon = \varepsilon^e + \varepsilon^p \quad (12)$$

$$\varepsilon^e = \frac{1 + \nu}{E_0} \left(\frac{\sigma}{1 - D} \right) - \frac{\nu}{E_0} \frac{Tr(\sigma)}{1 - D} \quad (13)$$

The potential function is chosen as follow

$$\tilde{g} = \tilde{g} \left(J(\tilde{\sigma} - \alpha) - R - k + \frac{3\zeta}{4h} \alpha : \alpha \right) \quad (14)$$

The governing equations of constitutive model coupled with the damage are listed as follows

$$d\varepsilon^p = d\lambda \frac{\partial \tilde{g}}{\partial \sigma} = \frac{3}{2} d\lambda \frac{\tilde{\sigma} - \alpha}{J_2(\tilde{\sigma} - \alpha)} \frac{1}{1 - D} \quad (15)$$

$$dX = -d\lambda \frac{\partial \tilde{g}}{\partial \alpha} = \frac{3}{2} d\lambda \frac{\tilde{\sigma} - \alpha}{J_2(\tilde{\sigma} - \alpha)} - \frac{3\zeta}{2h} \alpha d\lambda = (1 - D) d\varepsilon^p - \frac{3\zeta}{2h} \alpha d\lambda \quad (16)$$

$$dr = -d\lambda \frac{\partial \tilde{g}}{\partial R} = d\lambda \quad (17)$$

$$dp = \left(\frac{2}{3} d\varepsilon^p : d\varepsilon^p \right)^{\frac{1}{2}} = \frac{d\lambda}{1 - D} \quad (18)$$

$$d\alpha = \frac{2}{3} h(1 - D) d\varepsilon^p - \zeta \alpha dp(1 - D) \quad (19)$$

α is regarded as the deviator part of back stress. It is appropriate to decompose α into several parts in terms of the report of Chaboche (2008)

$$\alpha = \sum_{i=1}^M \alpha^{(i)} \quad (20)$$

Where, M denotes the number of parts of back stress. Moreover, we can justify consider strain hardening, dynamic recovery and fatigue damage for each $\alpha^{(i)}$

$$\dot{\alpha}^{(i)} = \frac{2}{3} h^{(i)} \dot{\varepsilon}^p - \zeta^{(i)} \alpha^{(i)} \dot{p}^{(i)} (1 - D) \quad (21)$$

Where $h^{(i)}$ and $\zeta^{(i)}$ are the material parameters for strain hardening and dynamic recovery respectively, and $\dot{p}^{(i)}$ is plastic strain rate being the dynamic recovery of $\alpha^{(i)}$. If $\dot{p}^{(i)} = \dot{p}$ and $D = 0$, Eq. (22) is degraded into the Armstrong and Frederick form model.

3.4 LCF Isotropic hardening coupled with fatigue damage

The yield surface is enlarged or reduced during cyclic loading process. The stress amplitude of LCF comprises the back stress, isotropic hardening stress and yield stress. Its evolution can be described by scalars R and k . R represents the variation of radius of yield surface. The isotropic hardening/softening rule is described as follows

$$dR = b(R_\infty - R)\dot{\lambda} \quad (22)$$

If considering isotropic damage of fatigue, it is rewritten as

$$dR = b(R_\infty - R)(1 - D)dp \quad (23)$$

Or $R = R_\infty[1 - \exp(-bp(1 - D))]$

Owing to the influence of load amplitude of LCF, the parameters of isotropy are not fixed. In the case of different strain amplitude of LCF, the R_∞ is a function of q , ($q = \frac{1}{2}\Delta\varepsilon_{p\max}$)

$$R_\infty = R_M - (R_M - R_0)\exp(-2\mu q) \quad (24)$$

Where, R_M , R_0 and μ are constant.

3.5 Discretization and integration

Backward Euler method is used to solve the group of differential equations in a cycle which is applied in the work of Yu *et al.* (2012). According to the Eqs. (12)-(24), the interval from a state n to $n + 1$ is considered into the method which allows the equations to be discretized as

$$\varepsilon_{n+1} = \varepsilon_{n+1}^e + \varepsilon_{n+1}^p \quad (25)$$

$$\varepsilon_{n+1}^p = \varepsilon_n^p + \Delta\varepsilon_{n+1}^p \quad (26)$$

$$\sigma_{n+1} = (1 - D)D^e : (\varepsilon_{n+1} - \varepsilon_{n+1}^p) \quad (27)$$

$$\Delta\varepsilon_{n+1}^p = \sqrt{\frac{3}{2}}\Delta p_{n+1}n_{n+1} \quad (28)$$

$$n_{n+1} = \sqrt{\frac{3}{2}}\frac{s_{n+1} - \alpha_{n+1}}{Y_{n+1}} \quad (29)$$

$$F_{n+1} = \frac{3}{2}(s_{n+1} - \alpha_{n+1}) : (s_{n+1} - \alpha_{n+1}) - Y_{n+1}^2 \quad (30)$$

$$\alpha_{n+1} = \sum_{i=1}^M \alpha_{n+1}^{(i)} \quad (31)$$

$$\alpha_{n+1}^{(i)} = \alpha_n^{(i)} + \left(\frac{2}{3}h^{(i)}\Delta\varepsilon_{n+1}^p - \zeta^{(i)}\alpha_{n+1}^{(i)}\Delta p_{n+1}^{(i)} \right)(1 - D) \quad (32)$$

$$\Delta R_{n+1} = b(R_\infty - R_n)(1 - D)\Delta p_{n+1} \quad (33)$$

$$Y_{n+1} = (Y_n + \Delta R_{n+1})(1 - D) \quad (34)$$

All constitutive variables at n and $\Delta\varepsilon_{n+1}$ are given firstly to find σ_{n+1} satisfying the discretized constitutive relations from Eq. (25) to Eq. (34). We use return mapping method given by Simo and Taylor (1985) consisting of an elastic predictor and a plastic corrector. The fatigue damage is supposed to be constant in a cycle. The elastic predictor is taken to be an elastic tentative stress

$$\sigma_{n+1}^* = (1-D)D^e : (\varepsilon_{n+1} - \varepsilon_n^p) \quad (35)$$

The yield condition is as follow

$$F_{n+1}^* = \frac{3}{2} (s_{n+1}^* - \alpha_n) : (s_{n+1}^* - \alpha_n) - Y_n^2 \quad (36)$$

here s_{n+1}^* is the deviatoric part of σ_{n+1}^* .

If $F_{n+1}^* \geq 0$, σ_{n+1} is the on the yield surface ($F_{n+1} = 0$) and expressed as follows

$$\sigma_{n+1} = \sigma_{n+1}^* - (1-D)D^e : \Delta\varepsilon_{n+1}^p \quad (37)$$

Where, $D^e : \Delta\varepsilon_{n+1}^p$ is the plastic corrector. Taking the deviatoric part of the above equation, and Eqs. (31, 32) are introduced to it with the fatigue damage parameter D

$$s_{n+1} - \alpha_{n+1} = s_{n+1}^* - (1-D)G\Delta\varepsilon_{n+1}^p - \sum_{i=1}^M \varepsilon_{n+1}^p \quad (38)$$

$$G = \frac{E}{2(1+\nu)} \quad (39)$$

G represents the plastic shear modulus.

The back stress $\alpha_{n+1}^{(i)}$ is obtained from Eq. (32) as

$$\alpha_{n+1}^{(i)} = \theta_{n+1}^{(i)} \left(\alpha_n^{(i)} + \frac{2}{3} h^{(i)} \Delta\varepsilon_{n+1}^p \right) \quad (40)$$

Where: $\theta_{n+1}^{(i)}$ is defined by the following equation and satisfies $0 < \theta_{n+1}^{(i)} \leq 1$ with introducing fatigue damage D

$$\theta_{n+1}^{(i)} = \frac{1}{1 + (1-D)\zeta^{(i)} \Delta p_{n+1}^{(i)}} \quad (41)$$

Elimination of $\Delta\varepsilon_{n+1}^p$ in Eqs. (32) and (38) using Eq. (40) gives

$$s_{n+1} - \alpha_{n+1} = \frac{Y_{n+1} \left(s_{n+1}^* - \sum_{i=1}^M \theta_{n+1}^{(i)} \alpha_n^{(i)} \right)}{Y_{n+1} + \left[3G(1-D) + \sum_{i=1}^M \theta_{n+1}^{(i)} h^{(i)} \right] \Delta p_{n+1}} \quad (42)$$

Then application of Eq. (42) into the yield condition $F_{n+1} = 0$ provides

$$\Delta p_{n+1} = \frac{\left[\frac{3}{2} \left(s_{n+1}^* - \sum_{i=1}^M \theta_{n+1}^{(i)} \alpha_n^{(i)} \right) : \left(s_{n+1}^* - \sum_{i=1}^M \theta_{n+1}^{(i)} \alpha_n^{(i)} \right) \right]^{1/2}}{3G(1-D) + \sum_{i=1}^M \theta_{n+1}^{(i)} h^{(i)}} - Y_{n+1} \quad (43)$$

The Eq. (43) gives out expression to calculate a scalar Δp_{n+1} . The consistent tangent modulus is given as follows in term of the Eq. (19) with consideration fatigue damage

$$d\Delta\sigma_{n+1} = D^e : \left(d\Delta\Delta_{n+1} - d\Delta\Delta\varepsilon_{n+1}^p \right) (1-D) \quad (44)$$

Combining the Eqs. (25)-(32), the explicit expression is

$$\frac{d\Delta\Delta_{n+1}}{d\Delta\Delta_{n+1}} = \left(D^e - 4G^2 L_{n+1}^{-1} : I_d \right) (1-D) \quad (45)$$

where

$$L_{n+1} = 2GI - \sum_{i=1}^M H_{n+1}^{(i)} + \frac{2}{3} \left(\frac{dY}{dp} \right)_{n+1} n_{n+1} \otimes n_{n+1} + \frac{2}{3} \frac{Y_{n+1}}{\Delta p_{n+1}} (I - n_{n+1} \otimes n_{n+1}) \quad (46)$$

$$I_d = I - \frac{1}{3} (1 \otimes 1) \quad (47)$$

For the A-F model in Eq. (21), the $H_{n+1}^{(i)}$ can be expressed as

$$H_{n+1}^{(i)} = \theta_{n+1}^{(i)} \left(\frac{2}{3} h^{(i)} I - \sqrt{\frac{2}{3}} \zeta^{(i)} a_{n+1}^{(i)} \otimes n_{n+1} \right) \quad (48)$$

4. Identification and verification

Simulation parameters of A42 for hysteresis loops and damage parameters are determined by test results by referring the method in reports of Lemaitre and Chaboche (1990), Kobayashi and Ohno (2002), Huang *et al.* (2011). The parameter values are listed in the Table 2.

The time independent constitutive relation (Eqs. (12)-(24)) coupled with fatigue damage (Eq. (11)) seems to be capable to estimate the hysteresis loops. Fig. 6 is the fatigue damage evolution for 0.8% and 0.6% strain amplitude. The estimation of fatigue damage model (Eq. (11)) seems

Table 2 Parameters for A42 LCF simulation

ζ_1	ζ_2	ζ_3	ζ_4	ζ_5	r_1 (MPa)	r_2 (MPa)	r_3 (MPa)
821	374	200	150	84	74	33	20
r_4 (MPa)	r_5 (MPa)	σ_0 (MPa)	E (GPa)	Q (MPa)	B	a	β
28	59	210	205	35.2	5	0.12	3.5

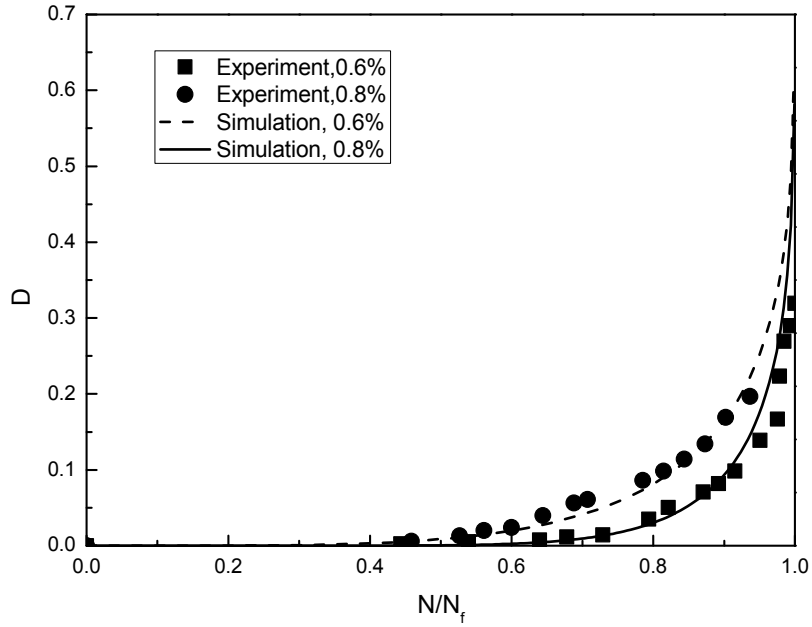


Fig. 6 Evaluation of stress amplitude evolution in LCF for A42 (strain amplitude: 0.6%, 0.8%, room temperature)

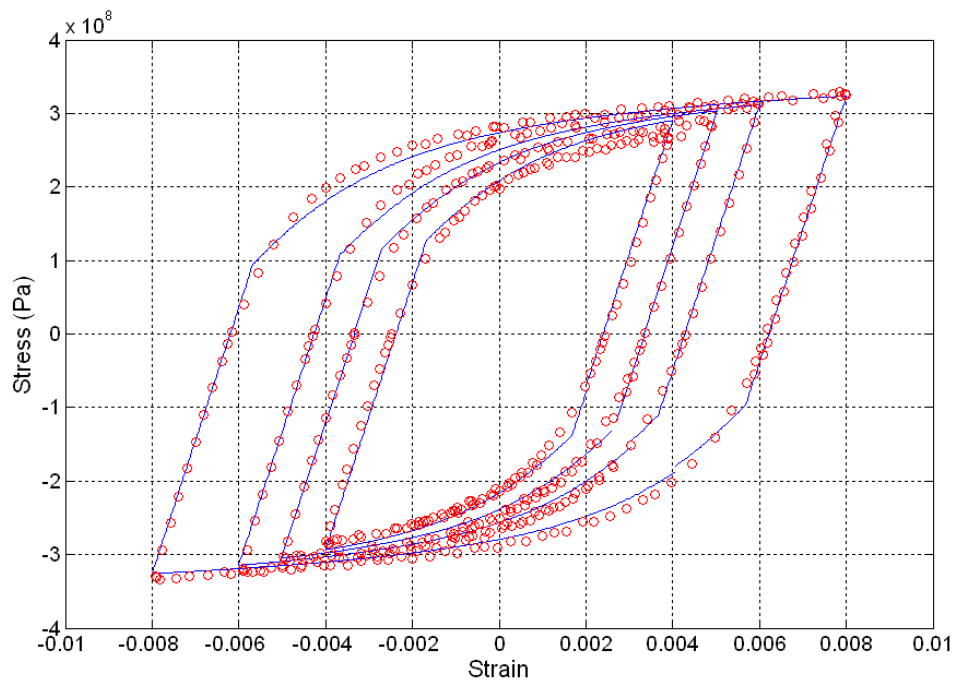


Fig. 7 A42, 0.1Hz, 20°, 2nd cycles, stress versus strain at 0.8%, 0.6%, 0.5%, 0.4%

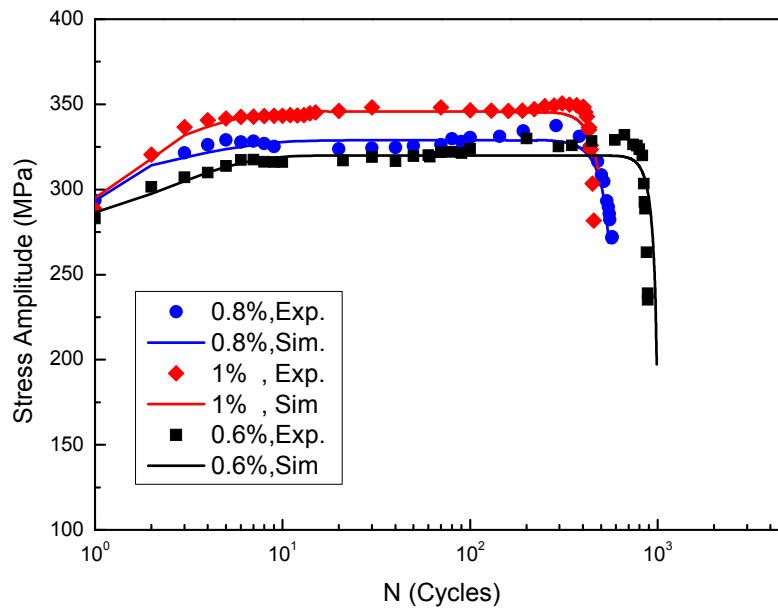


Fig. 8 Evaluation of stress amplitude evolution in LCF for A42 (room temperature)

to be good for it. The experimental points and the simulations of the second hysteresis loop are plotted in the Fig. 7 to compare for A42 at different strain amplitude 0.8%, 0.6%, 0.5%, 0.4% with 0.1 Hz.

A42 at RT has the isotropy hardening effect in the onset of the cycles; nevertheless the damage of fatigue decreases the stress amplitude after cyclic saturation which indicates the crack initiated and nucleated process. The simulation results show that the curve of cyclic stress amplitude with the experimental results in Fig. 8. The stress amplitude decreasing before failure caused by fatigue damage is well reflected in the model coupled with fatigue damage.

5. Conclusions

The C-Mn steel A42 has been investigated on the fatigue and damage behavior at room temperature. The constitutive theory coupled with the fatigue damage model is applied to describe the fatigue plastic deformation in macroscope. The Euler backward method is used to integrate the discretized differential equations and the return mapping method is applied to calculate the stress tensor through elastic predictor and plastic corrector terms. The simulation results of stress versus strain loops and cyclic stress evolution are good agreement with LCF test results in ambient temperature.

Acknowledgments

The research described in this paper was financially supported by the Natural Science

Foundation of China (No. 51101107 and No. 11372201).

References

- Armstrong, P.J. and Frederick, C.O. (1966), "A mathematical representation of the multiaxial bausinger effect", CEGB Report No. RD/B/N 731.
- Chaboche, J.L. (1987), "Continuum damage mechanics: Present state and future trends", *Nucl. Eng. Des.*, **105**(1), 19-33.
- Chaboche, J.L. (2008), "A review of some plasticity and viscoplasticity constitutive theories", *Int. J. Plast.*, **24**(10), 247-302.
- Chaboche, J.L., Kaminski, M. and Kanoute, P. (2009), "Extension and application of a non-linear fatigue damage accumulation rule for variable amplitude loading programs", *Deutscher Verband für Materialforschung und prufung e.V.*, pp. 627-639.
- Chopra, O.K. and Shack, W.J. (2002), "Review of the margins for ASME code fatigue design curve – Effects of surface roughness and material variability", Report of Argonne National Laboratory, Argonne National Laboratory, Lemont, IL, USA.
- Huang, Z.Y., Wagner, D., Bathias, C. and Chaboche, J.-L. (2011), "Cumulative fatigue damage in low cycle fatigue and gigacycle fatigue for low carbon–manganese steel", *Int. J. Fatigue.*, **33**(2), 115-121.
- Kobayashi, M. and Ohno, N. (2002), "Implementation of cyclic plasticity models based on a general form of kinematic hardening", *Int. J. Numer. Meth. Eng.*, **53**(9), 2217-2238.
- Le Duff, J.A., Lehericy, Y., Lefrançois, A. and Mendez, J. (2009), "Effects of surface finish and LCF pre-damage on the HCF endurance limits of A 304L austenitic stainless steel", *Deutscher Verband für Materialforschung und prufung e.V.*, Berlin, German, May.
- Lemaitre, J. and Chaboche, J.-L. (1990), *Mechanics of Solid Materials*, Cambridge University Press, Cambridge, UK.
- Liakat, M. and Khonsari, M.M. (2014), "An experimental approach to estimate damage and remaining life of metals under uniaxial fatigue loading", *Mater. Des.*, **57**, 289-297.
- Ohno, N., Tsuda, M. and Kamei, T. (2013), "Elastoplastic implicit integration algorithm applicable to both plane stress and three-dimensional stress states", *Finite. Elem. Anal. Des.*, **66**, 1-11.
- Rabotnov, Y.N. (1969), *Creep Problems in Structural Members*, North Holland Publishing Comp., London, UK.
- Simo, J.C. and Taylor, R.L. (1985), "Consistent tangent operators for rate-independent elastoplasticity", *Meth. Appl. Mech. Eng.*, **48**(1), 101-118.
- Yu, D., Chen G., Yu W., Li D. and Chen X. (2012), "Visco-plastic constitutive modeling on Ohno–Wang kinematic hardening rule for uniaxial ratcheting behavior of Z2CND18.12N steel", *Int. J. Plast.*, **28**(1), 88-101.

CC